Atmospheric
Chemistry
and Physics

Efficient bulk mass accommodation and dissociation of N_2O_5 in neutral aqueous aerosol

Goran Gržinić[1,2], Thorsten Bartels-Rausch[1], Andreas Türler[2,3], and Markus Ammann[2]

[1]Laboratory of Environmental Chemistry, Paul Scherrer Institut, Villigen, 5232, Switzerland
[2]Department of Chemistry and Biochemistry, University of Bern, Bern, 3012, Switzerland
[3]Laboratory of Radiochemistry, Paul Scherrer Institut, Villigen, 5232, Switzerland
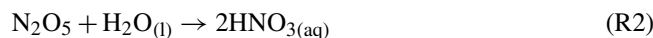
Correspondence to: Markus Ammann (markus.ammann@psi.ch)

Abstract. An isotope exchange experiment with the short-lived radioactive tracer ^{13}N is used to trace N_2O_5 uptake into nitrate-containing aqueous aerosol particles. While uptake of ^{13}N-labelled N_2O_5 to deliquesced Na_2SO_4 aerosol is consistent with previous studies, efficient exchange of labelled nitrate with the non-labelled nitrate pool was observed in the presence of aerosol-phase nitrate. The experiments provide direct evidence for efficient bulk mass accommodation of N_2O_5 into aqueous solution with $\alpha_b > 0.4$ at room temperature, as well as for the fast dissociation into nitronium and nitrate. While for experimental reasons this study is limited to non-acidic nitrate-containing aerosol, it is likely that bulk mass accommodation and dissociation are not limiting N_2O_5 uptake under wider ranges of conditions.

1 Introduction

The central role of NO_x in the regulation of the oxidative capacity of the atmosphere is well established. N_2O_5, an important species of the night-time chemistry of nitrogen oxides, has been identified as one of the major reservoir species and potential sinks of NO_x (Abbatt et al., 2012; Chang et al., 2011). NO_2 reacts with O_3 to form NO_3, which then react together to form N_2O_5 (Reaction R1).

$$NO_2 + NO_3 \rightleftarrows N_2O_5 \tag{R1}$$

Depending on location, N_2O_5 may be removed primarily by heterogeneous hydrolysis to nitric acid or other products on aerosol surfaces, thus providing a night-time sink for atmospheric NO_x (Reaction R2) (Abbatt et al., 2012; Chang et al.,

2011).

$$N_2O_5 + H_2O_{(l)} \rightarrow 2HNO_{3(aq)} \tag{R2}$$

Removal of N_2O_5 leads to a reduction of atmospheric NO_x and consequent reduction of tropospheric ozone and thus the oxidative capacity of the atmosphere (Dentener and Crutzen, 1993; Evans and Jacob, 2005). The reactivity of N_2O_5 with aerosols has been of ongoing interest for the past 2 decades. Laboratory investigations have encompassed measurement of uptake kinetics to a wide array of inorganic aerosols, like H_2SO_4/sulfates (Hallquist et al., 2003; Hanson and Lovejoy, 1994), NaCl/marine aerosol (Gaston and Thornton, 2016; George et al., 1994; Thornton and Abbatt, 2005), nitrate-containing inorganic aerosol (Hallquist et al., 2003; Mentel et al., 1999; Wahner et al., 1998) and mineral dust (Karagulian et al., 2006; Wagner et al., 2008). Further constraints have also been derived from field observations of N_2O_5 and aerosol abundance and composition (Bertram et al., 2009; Phillips et al., 2016). The uptake coefficient γ (defined as the probability that a gas kinetic collision of a molecule leads to its uptake at the interface) on deliquesced inorganic aerosol is in the 10^{-1}–10^{-2} range. Organic aerosol, in contrast, presents a wider range of reactivities, with values approaching those of inorganic aerosols in certain cases, such as for malonic acid (Griffiths et al., 2009; Thornton et al., 2003) at around 10^{-2}, while in other cases the uptake coefficients go down to 10^{-3}–10^{-5}, such as for some polycarboxylic acids like citric acid (Gržinić et al., 2015), succinic acid or humic acid (Badger et al., 2006; Griffiths et al., 2009), long-chained fatty acids, and polyalcohols (Gross et al., 2009) that indicate varying effects of water content and viscosity on the reactiv-
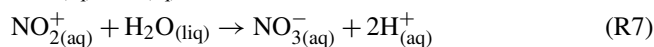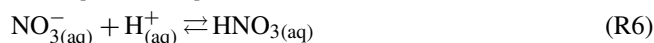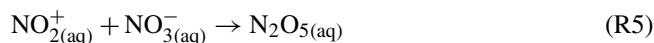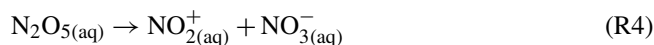
ity and kinetic regime. Additionally, coating aqueous particles with insoluble organic films has been shown to have an inhibiting effect on N_2O_5 uptake (Anttila et al., 2006; Folkers et al., 2003) by restricting transport from the gas phase to the aerosol phase, reduced solubility in the organic phase or limited water availability. The hydrolysis of $N_2O_5(g)$ is believed to proceed through a multistep process (Behnke et al., 1997; Mozurkewich and Calvert, 1988): molecular solvation (Reaction R3) is followed by dissociation into nitronium (NO_2^+, or its hydrated form $H_2ONO_2^+$) and nitrate (Reaction R4) with a rate coefficient, k_4, estimated to fall between 10^5 and $10^7 \, s^{-1}$ (Mentel et al., 1999; Bertram and Thornton, 2009; Griffiths et al., 2009). The fate of nitronium is governed by a competition between the reaction with nitrate to yield molecular N_2O_5 again (Reaction R5) with a nearly collision-limited rate coefficient, k_5, of $2.4 \times 10^{10} \, M^{-1} \, s^{-1}$ (Mentel et al., 1999), the reaction with $H_2O(l)$ to yield HNO_3 (Reaction R7) (k_5, between 10^7 and $10^9 \, M^{-1} \, s^{-1}$; Mentel et al., 1999; Behnke et al., 1997) and reactions with other nucleophiles (such as chloride ion) not considered further here.

$$N_2O_{5(g)} \rightleftharpoons N_2O_{5(aq)} \tag{R3}$$

$$N_2O_{5(aq)} \rightarrow NO_{2(aq)}^+ + NO_{3(aq)}^- \tag{R4}$$

$$NO_{2(aq)}^+ + NO_{3(aq)}^- \rightarrow N_2O_{5(aq)} \tag{R5}$$

$$NO_{3(aq)}^- + H_{(aq)}^+ \rightleftharpoons HNO_{3(aq)} \tag{R6}$$

$$NO_{2(aq)}^+ + H_2O_{(liq)} \rightarrow NO_{3(aq)}^- + 2H_{(aq)}^+ \tag{R7}$$

The elementary reactions constituting this mechanism have been suggested based on the kinetic behaviour as a function of a range of conditions, but they have not been unambiguously proven by detecting, e.g. NO_2^+ directly. As long as nitrate is a minority species in the aerosol phase, the loss of N_2O_5 is driven by Reaction R7. Depending on the water content, either the transfer of N_2O_5 into the aqueous phase, Reaction R3 (also referred to as mass or bulk accommodation), the dissociation (Reaction R4) or Reaction R7 are rate limiting according to current understanding (Abbatt et al., 2012).

However, in the presence of significant amounts of nitrate in the aqueous phase, the loss of nitronium ion by reaction with nitrate back to N_2O_5, Reaction R5, becomes significant, and the uptake of N_2O_5 becomes lower with increasing nitrate content in the aerosol phase, typically by an order of magnitude. This effect is referred to as the "nitrate effect" (Abbatt et al., 2012; Bertram and Thornton, 2009; Hallquist et al., 2003; Mentel et al., 1999; Wahner et al., 1998).

Most studies conducted related to N_2O_5 reactivity with aqueous aerosol so far were based on measuring the net gas-phase loss of N_2O_5 due to uptake on an aerosol. The kinetics were described with a simplified lumped mechanism by assigning an effective Henry's law constant, H, of N_2O_5 of about 2 to 5 $M \, atm^{-1}$ at room temperature and a net rate coefficient for the overall reaction of N_2O_5 with H_2O to HNO_3, k_0^{II}, of around $10^5 \, M^{-1} \, s^{-1}$ (Ammann et al., 2013; Bertram and Thornton, 2009; Griffiths et al., 2009), so that the uptake

coefficient can be described via the resistor model as given by Eq. (1).

$$\frac{1}{\gamma} = \frac{1}{\alpha_b} + \frac{c}{4HRT\sqrt{D_l k^{II} [H_2O]} \left[\coth(r/l) - (l/r) \right]}$$

$$l = \sqrt{\frac{D_l}{k^{II} [H_2O]}}, \tag{1}$$

where α_b denotes the bulk mass accommodation coefficient, c the mean thermal velocity of N_2O_5 in the gas phase, D_l the diffusion coefficient of N_2O_5 in the aqueous phase, usually set to $10^{-5} \, cm^2 \, s^{-1}$ for low-viscosity aqueous aerosol, $[H_2O]$ the concentration of H_2O in M, r the particle radius and l the reacto-diffusive length. The apparent levelling off of γ towards high relative humidity (RH) was explained by a limiting α_b of about 0.03 (Ammann et al., 2013) or by introducing a dependence of the dissociation rate, k_4, on the water content, leading to an apparent water content dependence of k_0^{II} (Bertram and Thornton, 2009). The effect of nitrate as mentioned above has been taken into account by using Eq. (2) instead of a fixed rate coefficient k_0^{II}:

$$k^{II} = k_0^{II} \left(1 - \frac{1}{1 + \frac{k_7 [H_2O]}{k_5 [NO_3^-]}} \right). \tag{2}$$

This expression requires the knowledge of the concentrations of water and nitrate and the ratio of the two rate coefficients k_7/k_5, for which values between 0.02 and 0.06 lead to reasonable consistency with available data (Ammann et al., 2013; Bertram and Thornton, 2009). However, the actual size of the pool of dissolved N_2O_5 (or its dissociated products NO_2^+ and NO_3^-), the true value of the bulk mass accommodation coefficient, α_b, and the rate coefficients for the individual reactions have remained elusive. In this study, we make specific use of the short-lived radioactive isotope ^{13}N (Ammann, 2001; Gržinić et al., 2015, 2014) to trace the exchange of ^{13}N-labelled nitrate resulting from uptake of labelled N_2O_5 with the non-labelled nitrate pool in the aerosol phase. This allows us to obtain a direct estimate of α_b and constraints for the N_2O_5 dissociation (Reaction R4) and the recombination reaction (Reaction R5). The tracer method is very sensitive in detecting phase transfer of labelled N_2O_5 at very low gas-phase concentrations and thus is able to escape any artefact nitrate effect due to build-up of nitrate during the course of a kinetic experiment for experiments with aerosol without any nitrate initially as discussed by Gržinić et al. (2015). However, this sensitivity comes at the expense of chemical selectivity in the sense that re-evaporating HNO_3 product from an acidic aerosol would interfere with the N_2O_5 measurement as shown in our previous study (Gržinić et al., 2014). We therefore performed the experiments presented here with neutral sodium sulfate and sodium nitrate aerosol to avoid this interference.

2 Experimental section

A detailed description of the experimental method and set-up can be found in our previous publications relating to the production of ^{13}N-labelled N$_2$O$_5$ (Gržinić et al., 2014) and uptake of N$_2$O$_5$ on citric acid aerosol (Gržinić et al., 2015). The short-lived radioactive tracer ^{13}N ($T_{1/2} \approx 10$ min) is produced via the ^{16}O(p,α)^{13}N reaction in a gas target by irradiating a 20 % O$_2$ in He flow with 11 MeV protons produced by the Injector II cyclotron at the Paul Scherrer Institute, Switzerland. The highly oxidized ^{13}N-labelled species are reduced to ^{13}NO for transport via a 580 m long PVDF capillary tube to the laboratory. Figure 1 shows a schematic of the experimental set-up used in this study. ^{13}NO-containing gas from the accelerator facility (50 mL min^{-1}) is mixed with ~ 3 mL min^{-1} of 10 ppmv non-labelled NO in N$_2$ from a certified gas cylinder and nitrogen carrier gas (only a very small fraction of NO is labelled with ^{13}N, about 10^{-6} and lower). This gas flow is mixed in the N$_2$O$_5$ synthesis reactor with a 50 mL min^{-1} flow containing ~ 8 ppmv O$_3$ produced by irradiating a 10 % O$_2$ in N$_2$ gas mixture with 185 nm UV light. The reactor is a glass tube of 34 cm length and 4 cm inner diameter, lined with PTFE foil and operated under dry conditions to minimize hydrolysis of N$_2$O$_5$ on the walls. The gas-phase chemistry of NO with O$_3$ results in the formation of NO$_2$, NO$_3$ and finally N$_2$O$_5$ (Reaction R1). The resulting gas flow is mixed with a secondary gas flow containing aerosol (720 mL min^{-1}) in an aerosol flow tube. This flow tube differs from the one that we used in our previous studies in that it is optimized for measurement of uptake coefficients in the 10^{-1}–10^{-2} range. It consists of a glass tube 39.3 cm in length and 1.4 cm in inner diameter. The inside of the glass tube is coated with halocarbon wax to minimize N$_2$O$_5$ losses to the wall by heterogeneous hydrolysis. A PTFE tube (6 mm diameter) is inserted coaxially into the flow tube to act as injector for the N$_2$O$_5$ flow. The injector contains holes at the end, which allow the N$_2$O$_5$ flow to be injected perpendicularly to the aerosol flow. Mixing is assumed to be rapid, and a laminar flow profile is assumed to have been established in the first few centimetres. A black shroud is used to cover the N$_2$O$_5$ synthesis reactor and the aerosol flow tube in order to prevent NO$_3$ photolysis and thus N$_2$O$_5$ loss. Aerosol is produced by nebulizing 0.1 %wt. NaNO$_3$, Na$_2$SO$_4$ and 1 : 1 NaNO$_3$ / Na$_2$SO$_4$ solutions in Milli-Q water. The resulting aerosol flow is dried over a Nafion membrane diffusion drier (RH of the drying gas outside is adjusted to 40 % RH to prevent efflorescence) and passed through an ^{85}Kr bipolar ion source and an electrostatic precipitator to equilibrate the charge distribution and subsequently remove the charged particles, respectively. A humidifier is placed after the ion source to adjust the humidity of the gas flow to the required experimental levels. The overall gas flow exiting from the aerosol fast-flow reactor is split into two flows via a T-connector, one of which is connected to an SMPS (scanning mobility particle sizer) system used to characterize the aerosol, consisting of a ^{85}Kr bipolar ion source to re-establish charge equilibrium, a differential mobility analyzer (DMA, TSI 3071) and a condensation particle counter (CPC, TSI 3022). The other part of the gas flow is directed into a parallel plate diffusion denuder system, where the various ^{13}N-containing gaseous species (N$_2$O$_5$, NO$_3$ and NO$_2$) are trapped by lateral diffusion and chemical reaction on a series of parallel, selectively coated aluminum plates: citric acid for trapping N$_2$O$_5$ and NO$_3$, a 1 : 1 mixture of NDA (N-(1-naphthyl)ethylene diamine dihydrochloride) and KOH for trapping NO$_2$. The aerosol particles, which have small diffusivity, pass without loss through the denuder system and are trapped on a glass fiber filter placed at the exit. The radioactive decay of ^{13}N is measured by placing a CsI scintillator crystal with PIN diode detectors (Caroll and Ramsey, USA) on each of the denuder traps and the particle filter. ^{13}N decays by β^+ decay, and the resulting positron annihilates with an electron with emission of two coincident γ rays in opposite directions. The resulting signal can be related to the concentration of the species in the gas and particle phase by comparing the NO$_2$ concentration measured with a NO$_x$ analyzer to the ^{13}NO$_2$ and ^{13}N$_2$O$_5$ signals on the denuder plates and particle filter, respectively. The gas-phase non-labelled NO$_2$ and N$_2$O$_5$ concentrations were around 10^{11} molecule cm^{-3}. The signal on the particle filter is related to aerosol-phase nitrate after removal of dissolved N$_2$O$_5$ by stripping the gas-phase N$_2$O$_5$ in the denuder system. The equilibrium established by Reactions R4 and R5 is fast enough to ensure that. In turn, the amount of dissolved N$_2$O$_5$ remains orders of magnitude smaller than the amount of nitrate built up in the particle phase along the flow tube, so that the net loss of N$_2$O$_5$ in the gas phase corresponds to the net gain of nitrate in the particle phase. Unfortunately, due to experimental limitations, only a limited number of measurements could be performed. The ^{13}N tracer technique is dependent on smooth operation of the accelerator facilities and constant online ^{13}N production to be successful, which is not always the case. Individual experiments involved the acquisition of data points consisting of 15–20 activity measurements, each integrated over 60 s, for a given injector position. Overall, replicates from several different experiment series performed on several different operation days of the ^{13}N delivering facility were averaged to obtain values and standard deviations reported in Table 1.
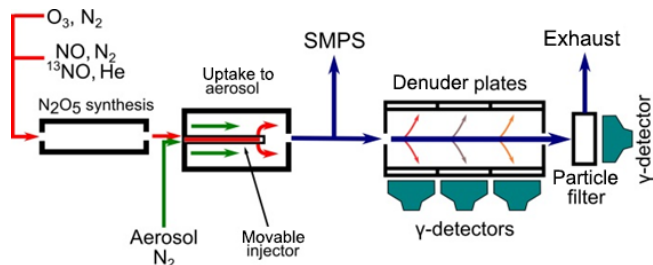
3 Results and discussion

The measurements were performed at 50 and 70 % RH for all three of the solutions in question. The operating procedure was similar to the one reported by Gržinić et al. (2015, 2014), although in the present case the experiment was performed by measuring the change in signals under variation of the position of the injector (reaction time) and not the ratio of aerosol surface to volume. Appropriate corrections have been applied to the N$_2$O$_5$ signal to account for NO$_2$ interference

Table 1. Experimental parameters and results. The corrected uptake coefficients of ^{13}N-labelled N$_2$O$_5$ are highlighted in bold.

Aerosol	NaNO$_3$	NaNO$_3$	NaNO$_3$/Na$_2$SO$_4$	NaNO$_3$/Na$_2$SO$_4$	Na$_2$SO$_4$	Na$_2$SO$_4$
Molar mixing ratio	–	–	1 : 1	1 : 1	–	–
Temperature (K)	295 ± 1	295 ± 1	295 ± 1	295 ± 1	295 ± 1	295 ± 1
RH (%)	50 ± 1	70 ± 1	51 ± 1	70 ± 1	51 ± 1	70 ± 1
Average S/V ratio (m^2 m^{-3})	5.66×10^{-3}	5.00×10^{-3}	3.36×10^{-3}	4.76×10^{-3}	3.42×10^{-3}	3.00×10^{-3}
γ^*_{eff} (^{13}NNO$_5$)	0.057	0.18	0.054	0.17	0.0052	0.025
Error[a]	± 0.004	± 0.02	± 0.008	± 0.02	± 0.002	± 0.003
γ^* (^{13}NNO$_5$)[b]	**0.067**	**0.29**	**0.063**	**0.26**	**0.0053**	**0.027**
Total error[c]	± 0.02	± 0.1	± 0.02	± 0.2	± 0.002	± 0.008
[H$_2$O] (M)[d]	28.5	38.2	34.4	41.6	38.6	43.8
[NO$_3^-$] (M)[d]	13.1	8.78	4.60	3.29	0	0
k_7[H$_2$O] $/k_5$[NO$_3^-$][e]	0.044	0.087	0.15	0.25	–	–
γ (non-labelled N$_2$O$_5$)[f]	0.0050	0.010	0.013	0.019	0.044	0.047

[a] 95 % confidence level of the fit of Eq. (3) to the data as shown in Fig. 2. [b] Corrected for diffusion in the gas phase. [c] Including 30 % uncertainty related to the ratio of aerosol surface to volume. [d] From AIM model (Clegg et al., 1998). [e] $k_7/k_5 = 0.02$. [f] Calculated using Eqs. (1) and (2), with $k_0^{\mathrm{II}} = 10^5$ M^{-1} s^{-1} and $H = 2$ M atm^{-1}.

Figure 1. Schematic of the experimental set-up.

on the denuder coating used for N$_2$O$_5$ (citric acid) as well as for the small amounts of NO$_3$ present in the gas phase, as described in our previous studies. Before each experimental run, a wall loss measurement was performed without aerosol by moving the injector in 5–10 cm steps along the length of the aerosol flow tube and measuring the gas-phase N$_2$O$_5$ signal in order to obtain the pseudo-first-order wall loss rate constants (k_{w}) for each experiment. These values varied between $\sim 3 \times 10^{-2}$ and $\sim 7 \times 10^{-2}$ s^{-1}, depending on humidity. The citric acid coating used to trap N$_2$O$_5$ in the denuder system is not able to differentiate N$_2$O$_5$ from HNO$_3$. However, any significant presence of HNO$_3$ formed along the walls upstream of the aerosol flow tube would have been noticed due to its very large wall loss rate coefficient (Guimbaud et al., 2002), which was not observed; the uptake coefficient for labelled N$_2$O$_5$ on the reactor walls calculated from k_{w} was in the range of 10^{-7}, which would not lead to substantial HNO$_3$ production. NO$_2$ concentrations in the system were measured by switching a NO$_x$ analyzer in place of the SMPS system at the beginning of the experiment. By comparing this result to the signals from ^{13}N-labelled N$_2$O$_5$ and NO$_2$, the concentration of non-labelled N$_2$O$_5$ in the system was also calculated, as described in our previous studies
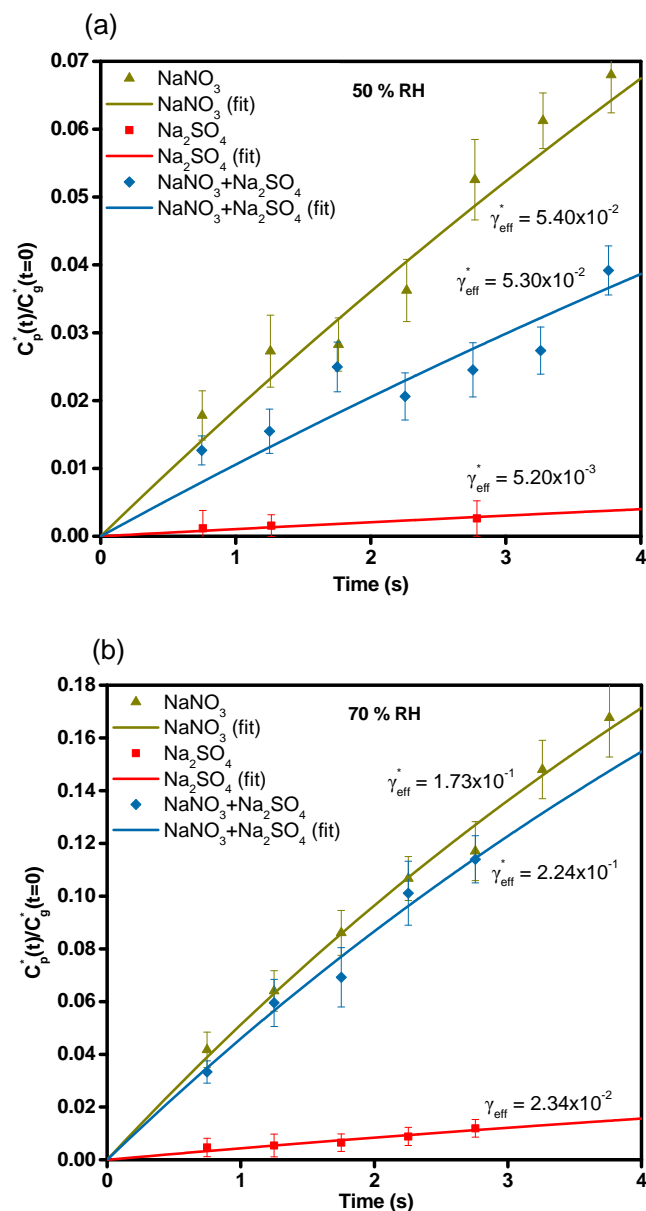
(Gržinić et al., 2015, 2014). The uptake measurements were performed in a similar fashion to the wall loss measurements, although in this case aerosol was introduced at each step. By using Eq. (3), which describes gas–aerosol-phase interaction kinetics, we can estimate the uptake coefficient.

$$\frac{C_{\mathrm{p}}^*(t)}{C_{\mathrm{g}}^*(t=0)} = \frac{1 - e^{-(k_{\mathrm{w}}+k_{\mathrm{p}})t}}{1 + \frac{k_{\mathrm{w}}}{k_{\mathrm{p}}}}, \tag{3}$$

$$k_{\mathrm{p}} = \frac{S_{\mathrm{p}} \omega \gamma^*_{\mathrm{eff}}}{4}, \tag{4}$$

where $C_{\mathrm{g}}^*(t=0)$ is the gas-phase labelled N$_2$O$_5$ concentration in molecules cm^{-3} at time zero, $C_{\mathrm{p}}^*(t)$ is the labelled particle-phase nitrate concentration expressed as number of particle-phase labelled nitrate ions per volume of gas phase, in ions cm^{-3}, k_{w} is the wall loss rate coefficient, measured as described above, and k_{p} denotes the apparent first-order rate coefficient for gas-phase loss of labelled N$_2$O$_5$ to the aerosol phase, which can be related to the effective uptake coefficient (γ^*_{eff}) of labelled N$_2$O$_5$ by Eq. (4), where S_{p} is the total ratio of the total particle surface area to gas volume of the aerosol and ω is the mean thermal velocity of N$_2$O$_5$. Figure 2 shows the appearance of ^{13}N in the aerosol phase as a function of time performed together with least-squares fits using Eq. (3) with γ^*_{eff} as the only variable. The true uptake coefficients were then obtained by correction for gas-phase diffusion of N$_2$O$_5$, as described by Pöschl et al. (2007), which leads to considerable corrections for uptake coefficients above 0.1 and particle diameters around 400 nm. The diffusion coefficient was taken as 0.085 cm^{-2} s^{-1} at ambient temperature and pressure (Tang et al., 2014).

Table 1 summarizes the results obtained for the various aerosols, experimental conditions, γ^*_{eff} as returned from the fits to the data and γ^* after the diffusion correction. In the absence of aerosol-phase nitrate, γ^* for Na$_2$SO$_4$ at 70 % RH

Figure 2. Normalized particle-phase labelled nitrate concentration vs. time for experiments performed at 50 % RH **(a)** and 70 % RH **(b)**. The data points represent the measurement data, the error bars represent the standard deviation of the measurements, and the curves are a least-squares fit of Eq. (1) to the measured data.

is comparable to that reported by Mentel et al. (1999). At 50 % RH, it is likely that the Na_2SO_4 particles remained effloresced (Gao et al., 2007) (the lowest RH in the aerosol conditioning system was 40 %), explaining the low γ of 0.0053, which is comparable to that previously reported for dry ammonium sulfate (Hallquist et al., 2003).
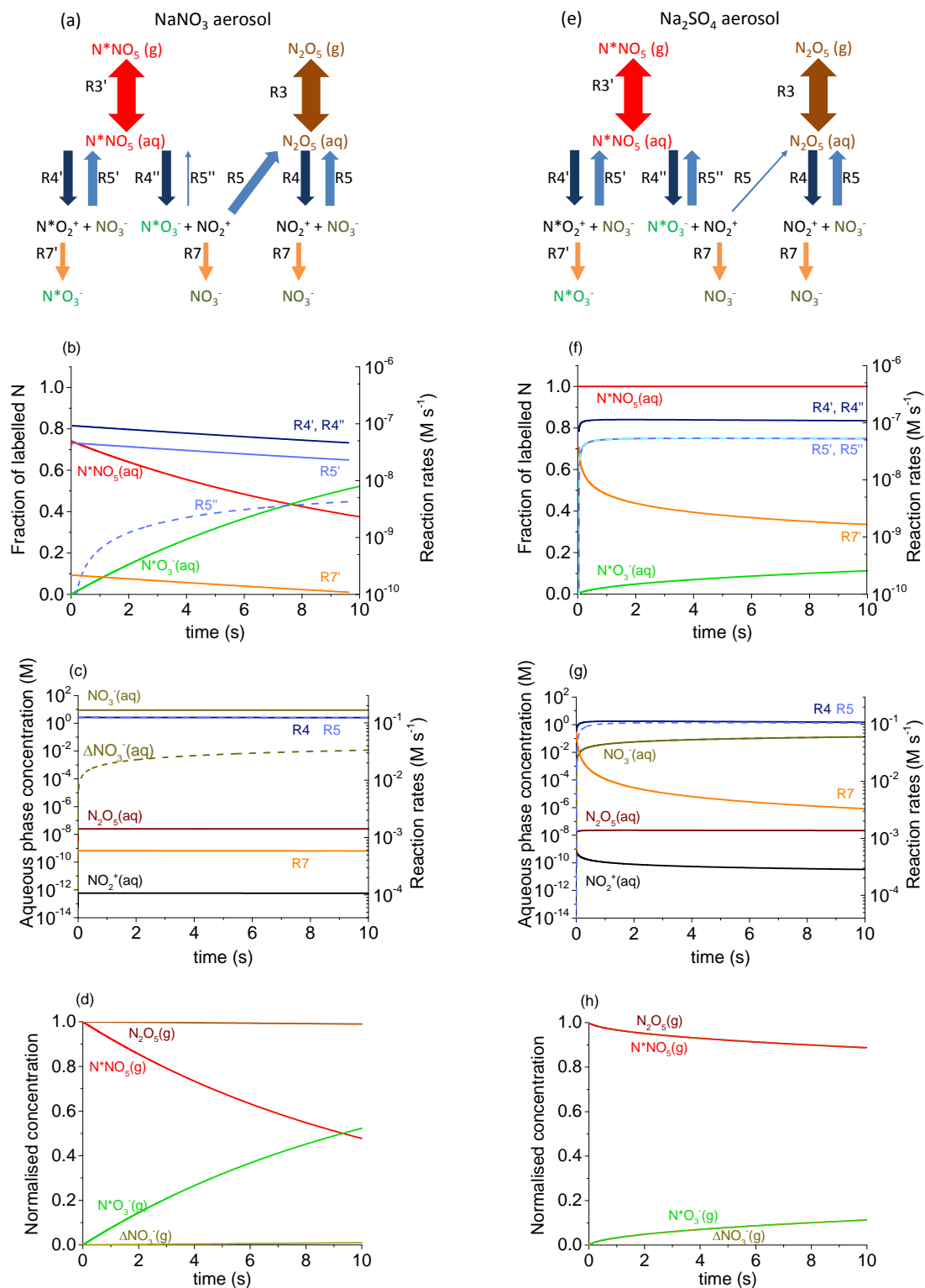
In the presence of aerosol-phase nitrate, uptake of ^{13}N-labelled N_2O_5 is drastically higher than the net uptake of non-labelled N_2O_5 observed in earlier studies (Bertram and

Thornton, 2009; Griffiths et al., 2009; Hallquist et al., 2003; Mentel et al., 1999; Wahner et al., 1998) or that predicted by the IUPAC-recommended expression (Ammann et al., 2013) also included in the table. A strong dependence of γ^* on humidity is observed, with an increase by a factor of about 3 from 50 to 70 % relative humidity. On mixed Na_2SO_4/$NaNO_3$ aerosol, the uptake is very close to that of pure $NaNO_3$ aerosol, at both humidities. Since the measured uptake coefficient for ^{13}N-labelled N_2O_5 into the nitrate-containing aerosol is about an order of magnitude larger than any uptake coefficient measured into not strongly acidic aqueous aerosol in previous studies, our results demonstrate that at room temperature gas–aqueous-phase exchange of N_2O_5 and its dissociation are very efficient, as also suggested by Mentel et al. (1999), based on experiments with $NaNO_3$, Na_2SO_4 and $NaHSO_4$ aerosol.

More insight into the interpretation of the present experiments with ^{13}N-labelled N_2O_5 can be obtained by deconvoluting the chemical mechanism of N_2O_5 hydrolysis (Reactions R3–R7) to take into account the fate of the labelled and non-labelled species separately. Assuming that the labelled N_2O_5 molecules contain only one ^{13}N atom (due to the very low labelled to non-labelled ratio of around 10^{-6} for the initial NO) and under the assumption that no isotopic effects are in play, the chemical mechanism can be assumed to proceed as shown in Fig. 3a.

We assume that upon dissociation of [13]NNO₅, there is an equal possibility that the ^{13}N label will end up either in the nitronium ion (NO_2^+) or in the nitrate ion (NO_3^-), with rate coefficients $k_4/2$. In the first scenario (right branch of the pathway for N*NO₅ in Fig. 3a) the ^{13}N label ends up on the nitrate ion (Reaction R4″). The corresponding non-labelled nitronium ion, if not reacting with H_2O (Reaction R7), reacts with the excess non-labelled nitrate to form non-labelled N_2O_5 (Reaction R5), while only a negligible fraction reacts with the labelled [13]NO_3^- (Reaction R5″). Thus, most of the labelled [13]NO_3^- is lost in the excess nitrate pool present in the aerosol. N_2O_5 re-evaporating to the gas phase is therefore non-labelled. Therefore, in this branch, all ^{13}N labels remain in the aqueous phase given that evaporation as HNO_3 is unlikely for our neutral aerosol. As evident from the experiments, the net transfer of labelled N_2O_5 into the aerosol nitrate pool, and thus the combination of bulk accommodation and dissociation, is very fast.

In the other scenario (left branch of N*NO₅ pathway in Fig. 3a) of the mechanism, ^{13}N ends up on the nitronium ion (Reaction R4′), and there are two possibilities for its further fate. The [13]NO_2^+ can react with water (Reaction R7′), bringing the label into the particulate nitrate pool. Alternatively [13]NO_2^+ can react with NO_3^- from the nitrate pool (Reaction R5′) to reform [13]NNO₅, which can eventually re-evaporate. Obviously, which of these two sub-channels are prevalent depends on water and nitrate concentrations as well as the rate coefficients of the two competing reactions.

Figure 3. (a) The chemical mechanism of N_2O_5 hydrolysis and chemical isotope exchange in nitrate-containing solutions. N* refers to ^{13}N. **(b, c, d)** Results of box model calculations for $NaNO_3$ aerosol at 70 % RH: evolution as a function of time of **(b)** the fraction of labelled N_2O_5 in the aqueous phase (red, left axis) and ratio of labelled nitrate to the total number of labelled N_2O_5 initially available (green, left axis); rates of reactions relevant for the budget of aqueous phase ^{13}N (light to dark blue, right axis); **(c)** rates of reactions relevant for the budget of non-labelled species in the aqueous phase; **(d)** evolution of normalized gas-phase N_2O_5 (labelled, red; non-labelled, brown) and aqueous-phase nitrate (labelled, green; non-labelled, olive) as a function of time. **(e, f, g, h)** Scheme and plots of the same quantities but for Na_2SO_4 aerosol at 70 % RH in the absence of pre-existing nitrate.

The water and nitrate concentrations for the conditions of the present experiments were derived from the AIM model (Clegg et al., 1998) and are also listed in Table 1. In the presence of nitrate, Reaction R5′ is the dominant pathway, as shown by Mentel et al. (1999) and Wahner et al. (1998), where values for the ratio k_5/k_7 of around 900 and 260, respectively, had been used as fitting parameters to explain the entirety of the nitrate effect.

In Fig. 3b, we report the results of box model calculations (described in the Supplement) for the scheme shown in Fig. 3a to substantiate these effects for NaNO$_3$ aerosol at 70 % RH. We have used the rate coefficients for $k_4 = 5 \times 10^6\,\mathrm{s^{-1}}$, $k_5 = 2.4 \times 10^{10}\,\mathrm{M^{-1}\,s^{-1}}$ and $k_7 = 2.6 \times 10^7\,\mathrm{M^{-1}\,s^{-1}}$ as suggested by Mentel et al. (1999) for NaNO$_3$ aerosol at various humidities; the bulk accommodation coefficient α_b was set to 1. Figure 3b (left y axis) directly demonstrates the rapid removal of labelled nitrogen from aqueous-phase N_2O_5 and its appearance as labelled nitrate. Parallel to that, labelled N_2O_5 disappears much more quickly from the gas phase and appears as aerosol-phase nitrate than non-labelled N_2O_5, as shown in Fig. 3d. It is also instructive to look at the rates of individual reactions contributing to the aqueous-phase budget of labelled species plotted in Fig. 3b and those of the non-labelled species in Fig. 3c: even though Reaction (R5′) brings back half of the labelled N_2O_5 (rate of Reaction R5′ is half of the dissociation rate; Fig. 3b), the fraction of labelled N_2O_5 drops below half of its initial value, since the exchange reactions R4 and R5 are fast, so that it may cycle through the aqueous-phase part of the scheme many times. The rate of Reaction R5″ (labelled nitrate with non-labelled nitronium) is not getting competitive, so that labelled nitrate remains in the nitrate pool.

The γ^* values calculated from the net N_2O_5 loss rates are about 0.26 for labelled N_2O_5, in good agreement with the value observed in the experiment, 0.29, and 0.0033 for non-labelled N_2O_5. The latter is consistent with the observation by Mentel et al. (1999) but lower than that suggested by the parameterization given in Eq. (1) based on the IUPAC recommendation and listed in Table 1 or that suggested by Bertram and Thornton (2009) or Griffiths et al. (2009) developed based on a wider dataset with other aerosol compositions. Box model simulation of the mixed salt case (not shown), also at 70 % RH, returns essentially the same results, 0.25 and 0.009, for the uptake coefficient of labelled and non-labelled N_2O_5, respectively, also in line with our measured γ^* of 0.26 for labelled N_2O_5.

The right column of Fig. 3 (e, f, g, h) presents the box model results for Na$_2$SO$_4$ aerosol at 70 % RH. The main difference is that in this case, Reaction (R5) represents only a negligible pathway for non-labelled nitronium resulting from Reaction (R4″), so that the majority of labelled nitrate recycles back to labelled N_2O_5 via Reaction (R5″). As a result, both labelled and non-labelled species behave exactly parallel, in terms of both rates and concentration. When solubility and rate coefficient are taken the same as those for the nitrate

aerosol, the magnitude of the calculated uptake coefficient is an order of magnitude too high. The difference between the kinetics described by Mentel et al. (1999) and Bertram and Thornton (2009) is that overall uptake is limited by the dissociation, k_4, in the latter, while Mentel et al. (1999) suggest faster dissociation and limitation by the interplay of the reactions of NO$_2^+$ with H$_2$O and NO$_3^-$. Replacing k_4 by the parameterization suggested by Bertram and Thornton, keeping k_5 as before but replacing k_7 such that $k_7/k_5 = 0.06$ as suggested by Bertram and Thornton, yields $\gamma = 0.06$, in reasonable agreement with the uptake coefficient measured here (0.027). However, this can also be achieved by the Mentel et al. (1999) kinetics scheme via lowering k_7 by 1 order of magnitude to achieve lower net uptake, which is what has been used in the calculations shown in Fig. 3f, g, h. In view of the limited dataset it is beyond the scope of this study to retrieve more precise rate coefficients for Reactions (R4), (R5) and (R7). The present results clearly indicate that accommodation and dissociation of N_2O_5 are not limiting net uptake for aerosol containing substantial amounts of nitrate. Furthermore, these experiments provide direct evidence that these elementary steps actually exist, because otherwise exchange with the non-labelled nitrate pool would not occur.

The measured uptake coefficient increases with RH (water content) as the increase in water concentration promotes the reaction of ^{13}NO$_2^+$ with water (Reaction R7′) while at the same time a decrease in nitrate concentration suppresses the ^{13}NNO$_5$ reformation sub-channel (Reaction R5′). However, as argued above, in the presence of nitrate at several M, the dominant fate of the label in the left branch of the mechanism in Fig. 3a is the reformation of labelled N_2O_5.

If bulk accommodation would limit uptake, the measured uptake coefficient would be only slightly larger than $\alpha_b/2$, with $\alpha_b/2$ contributed by the right branch of the mechanism, and a minor contribution from the left branch. Our results therefore strongly indicate that α_b must be at least about twice as high as the uptake coefficient of ^{13}N-labelled N_2O_5 measured for NaNO$_3$ and NaNO$_3$/Na$_2$SO$_4$ aerosols and thus $\alpha_b > 0.4$ when including the uncertainties related to the ratio of aerosol surface to volume and correction for gas-phase diffusion. In the box model simulations discussed above, α_b has been set to 1. The only systematic uncertainty not considered in this is the assumption that isotope effects do not influence the symmetry of the disproportionation reaction (Reaction R4).

Interestingly, the measured uptake coefficient is more sensitive to the water activity, irrespective of whether it is pure nitrate or mixed nitrate–sulfate particles, than to the fractional nitrate content. In spite of the fact that the expected ratio $k_7[\mathrm{H_2O}]/k_5[\mathrm{NO_3^-}]$ (see Table 1) increases substantially from pure nitrate to mixed nitrate–sulfate, still bulk accommodation and dissociation are not limiting, and the efficient exchange of the label with the non-labelled nitrate pool dominates the behaviour. Thus an increase of α_b, solubility in terms of salting effects, or of the rate of dissociation could ex-

plain the increase of the uptake coefficient of labelled N$_2$O$_5$ by a factor of 4 from 50 to 70 % RH. As discussed first by Mentel et al. (1999), and later by Griffiths et al. (2009) and Bertram and Thornton (2009), the kinetic regime may shift between limitations by Reactions (R7), (R4) or (R3) between low and high water activity, and it remains difficult to unambiguously assign the kinetic regime. Also from the present study, the evidence for the fast dissociation is very strong for the high nitrate mole fractions used, and we can only suggest that the dissociation is similarly fast for salt aerosol in the absence of nitrate.

On a side note, in principle, we cannot exclude a surface contribution. Since also the suggested bulk accommodation is followed by obviously very fast dissociation into nitronium and nitrate, this process will occur close to the surface anyhow, with a short reacto-diffusive length (in contrast to the much slower hydrolysis reaction of nitronium with H$_2$O). Therefore, for instance, varying the surface-to-volume ratio of the aerosol would not allow differentiating bulk from surface accommodation. However, we would prefer not invoking a surface process if bulk phase processing explains the observations.

Obviously, the fast isotope exchange that allows tracking the dissociation of dissolved N$_2$O$_5$ depends on the presence of a nitrate pool, which has to be substantial enough to "trap" the ^{13}N tracer and prevent its release. In other words, this method traces uptake of N$_2$O$_5$ into the non-limiting pool of aqueous nitrate. In the absence of nitrate, Reactions (R7$'$) and (R7) dominate in both branches (Fig. 3e), and the measured uptake coefficient for the ^{13}N-labelled N$_2$O$_5$ is comparable to that reported with other techniques for the same aerosol, in the range of a few 10^{-2} for Na$_2$SO$_4$ at 70 % RH in this study or for (NH$_4$)$_2$SO$_4$ reported by Gržinić et al. (2014), both consistent with available literature. For comparison, calculated uptake coefficients based on the parameterization and values from the IUPAC evaluation (Ammann et al., 2013), implemented in Eqs. (1) and (2), are also listed in Table 1.

4 Conclusion and atmospheric implications

Highly efficient uptake of ^{13}N-labelled N$_2$O$_5$ into nitrate-containing aqueous aerosol was observed and attributed to the exchange of ^{13}N-labelled nitrate as dissociation product of N$_2$O$_5$ with the nitrate pool in the aqueous phase. This allow us to suggest a very large value for the bulk mass accommodation coefficient for N$_2$O$_5$ into an aqueous aerosol at room temperature of $\alpha_b > 0.4$ at high relative humidity and fast dissociation at $> 10^6$ s^{-1}. This also provides direct evidence that the dissociation into nitrate and nitronium actually occurs and thus also supports the arguments behind the nitrate effect. The observed behaviour of ^{13}N-labelled N$_2$O$_5$ is similar to that observed by Wachsmuth et al. (2002), where $^{83–86}$Br isotopes have been used to determine the bulk accommodation coefficient of HOBr on aqueous bromide-

containing aerosol. The large value of α_b obtained for N$_2$O$_5$ at room temperature implies that other limiting processes must be at work to explain the insensitivity of the uptake coefficient to water content at high relative humidity (Abbatt et al., 2012; Griffiths et al., 2009; Thornton et al., 2003). Possible other aspects may be the temperature dependence of the solubility of N$_2$O$_5$ or salting effects as discussed in these previous studies, for which also strong indications come from this study to explain the strong water activity dependence of the observed uptake coefficient of ^{13}N-labelled N$_2$O$_5$. At least this study would exclude any accommodation limitation and supports previous indications that reaction and diffusion limit uptake of N$_2$O$_5$ to low-viscosity aqueous aerosol (Gržinić et al., 2015; Gaston and Thornton, 2016).

The Supplement related to this article is available online at doi:10.5194/acp-17-6493-2017-supplement.

References

Abbatt, J. P. D., Lee, A. K. Y., and Thornton, J. A.: Quantifying trace gas uptake to tropospheric aerosol: recent advances and remaining challenges, Chem. Soc. Rev., 41, 6555–6581, doi:10.1039/C2CS35052A, 2012.

Ammann, M.: Using ^{13}N as tracer in heterogeneous atmospheric chemistry experiments, Radiochim. Acta, 89, 831–838, 2001.

Ammann, M., Cox, R. A., Crowley, J. N., Jenkin, M. E., Mellouki, A., Rossi, M. J., Troe, J., and Wallington, T. J.: Evaluated kinetic and photochemical data for atmospheric chemistry: Volume VI

– heterogeneous reactions with liquid substrates, Atmos. Chem. Phys., 13, 8045–8228, doi:10.5194/acp-13-8045-2013, 2013.

Anttila, T., Kiendler-Scharr, A., Tillmann, R., and Mentel, T. F.: On the reactive uptake of gaseous compounds by organic-coated aqueous aerosols: Theoretical analysis and application to the heterogeneous hydrolysis of N_2O_5, J. Phys. Chem. A, 110, 10435–10443, 2006.

Badger, C. L., Griffiths, P. T., George, I., Abbatt, J. P. D., and Cox, R. A.: Reactive uptake of N_2O_5 by aerosol particles containing mixtures of humic acid and ammonium sulfate, J. Phys. Chem. A, 110, 6986–6994, 2006.

Behnke, W., George, C., Scheer, V., and Zetzsch, C.: Production and decay of $ClNO_2$, from the reaction of gaseous N_2O_5 with NaCl solution: Bulk and aerosol experiments, J. Geophys. Res., 102, 3795–3804, doi:10.1029/96jd03057, 1997.

Bertram, T. H. and Thornton, J. A.: Toward a general parameterization of N_2O_5 reactivity on aqueous particles: the competing effects of particle liquid water, nitrate and chloride, Atmos. Chem. Phys., 9, 8351–8363, doi:10.5194/acp-9-8351-2009, 2009.

Bertram, T. H., Thornton, J. A., Riedel, T. P., Middlebrook, A. M., Bahreini, R., Bates, T. S., Quinn, P. K., and Coffman, D. J.: Direct observations of N_2O_5 reactivity on ambient aerosol particles, Geophys. Res. Lett., 36, L19803, doi:10.1029/2009GL040248, 2009.

Chang, W. L., Bhave, P. V., Brown, S. S., Riemer, N., Stutz, J., and Dabdub, D.: Heterogeneous Atmospheric Chemistry, Ambient Measurements, and Model Calculations of N_2O_5: A Review, Aerosol Sci. Technol., 45, 665–695, doi:10.1080/02786826.2010.551672, 2011.

Clegg, S. L., Brimblecombe, P., and Wexler, A. S.: Thermodynamic model of the system H^+-NH_4^+-Na^+-SO_4^{2-}-NO_3^-- Cl^--H_2O at 298.15 K, J. Phys. Chem. A, 102, 2155–2171, 1998.

Dentener, F. J. and Crutzen, P. J.: Reaction of N_2O_5 on tropospheric aerosols: Impact on the global distributions of NO_x, O_3, and OH, J. Geophys. Res., 98, 7149–7163, doi:10.1029/92JD02979, 1993.

Evans, M. J. and Jacob, D. J.: Impact of new laboratory studies of N_2O_5 hydrolysis on global model budgets of tropospheric nitrogen oxides, ozone, and OH, Geophys. Res. Lett., 32, L09813, doi:10.1029/2005GL022469, 2005.

Folkers, M., Mentel, T. F., and Wahner, A.: Influence of an organic coating on the reactivity of aqueous aerosols probed by the heterogeneous hydrolysis of N_2O_5, Geophys. Res. Lett., 30, 1644, doi:10.1029/2003GL017168, 2003.

Gao, Y., Yu, L. E., and Chen, S. B.: Efflorescence Relative Humidity of Mixed Sodium Chloride and Sodium Sulfate Particles, J. Phys. Chem. A, 111, 10660–10666, 2007.

Gaston, C. J. and Thornton, J. A.: Reacto-Diffusive Length of N_2O_5 in Aqueous Sulfate- and Chloride-Containing Aerosol Particles, J. Phys. Chem. A, 120, 1039–1045, doi:10.1021/acs.jpca.5b11914, 2016.

George, C., Ponche, J. L., Mirabel, P., Behnke, W., Scheer, V., and Zetzsch, C.: Study of the Uptake of N_2O_5 by Water and NaCl Solutions, J. Phys. Chem., 98, 8780–8784, 1994.

Griffiths, P. T., Badger, C. L., Cox, R. A., Folkers, M., Henk, H. H., and Mentel, T. F.: Reactive Uptake of N_2O_5 by Aerosols Containing Dicarboxylic Acids. Effect of Particle Phase, Composition, and Nitrate Content, J. Phys. Chem. A, 113, 5082–5090, 2009.

Gross, S., Iannone, R., Xiao, S., and Bertram, A. K.: Reactive uptake studies of NO_3 and N_2O_5 on alkenoic acid, alkanoate, and polyalcohol substrates to probe nighttime aerosol chemistry, Phys. Chem. Chem. Phys., 11, 7792–7803, 2009.

Gržinić, G., Bartels-Rausch, T., Birrer, M., Türler, A., and Ammann, M.: Production and use of ^{13}N labeled N_2O_5 to determine gas–aerosol interaction kinetics, Radiochimica Acta, 102, 1025–1034, doi:10.1515/ract-2014-2244, 2014.

Gržinić, G., Bartels-Rausch, T., Berkemeier, T., Türler, A., and Ammann, M.: Viscosity controls humidity dependence of N_2O_5 uptake to citric acid aerosol, Atmos. Chem. Phys., 15, 13615–13625, doi:10.5194/acp-15-13615-2015, 2015.

Guimbaud, C., Arens, F., Gutzwiller, L., Gäggeler, H. W., and Ammann, M.: Uptake of HNO_3 to deliquescent sea-salt particles: a study using the short-lived radioactive isotope tracer ^{13}N, Atmos. Chem. Phys., 2, 249–257, doi:10.5194/acp-2-249-2002, 2002.

Hallquist, M., Stewart, D. J., Stephenson, S. K., and Cox, R. A.: Hydrolysis of N_2O_5 on sub-micron sulfate aerosols, Phys. Chem. Chem. Phys., 5, 3453–3463, 2003.

Hanson, D. R. and Lovejoy, E. R.: The Uptake of N_2O_5 onto Small Sulfuric-Acid Particles, Geophys. Res. Lett., 21, 2401–2404, 1994.

Karagulian, F., Santschi, C., and Rossi, M. J.: The heterogeneous chemical kinetics of N_2O_5 on $CaCO_3$ and other atmospheric mineral dust surrogates, Atmos. Chem. Phys., 6, 1373–1388, doi:10.5194/acp-6-1373-2006, 2006.

Mentel, T. F., Sohn, M., and Wahner, A.: Nitrate effect in the heterogeneous hydrolysis of dinitrogen pentoxide on aqueous aerosols, Phys. Chem. Chem. Phys., 1, 5451–5457, 1999.

Mozurkewich, M. and Calvert, J. G.: Reaction probability of N_2O_5 on aqueous aerosols, J. Geophys. Res., 93, 15889–15896, doi:10.1029/JD093iD12p15889, 1988.

Phillips, G. J., Thieser, J., Tang, M., Sobanski, N., Schuster, G., Fachinger, J., Drewnick, F., Borrmann, S., Bingemer, H., Lelieveld, J., and Crowley, J. N.: Estimating N_2O_5 uptake coefficients using ambient measurements of NO_3, N_2O_5, $ClNO_2$ and particle-phase nitrate, Atmos. Chem. Phys., 16, 13231–13249, doi:10.5194/acp-16-13231-2016, 2016.

Pöschl, U., Rudich, Y., and Ammann, M.: Kinetic model framework for aerosol and cloud surface chemistry and gas-particle interactions – Part 1: General equations, parameters, and terminology, Atmos. Chem. Phys., 7, 5989–6023, doi:10.5194/acp-7-5989-2007, 2007.

Tang, M. J., Cox, R. A., and Kalberer, M.: Compilation and evaluation of gas phase diffusion coefficients of reactive trace gases in the atmosphere: volume 1. Inorganic compounds, Atmos. Chem. Phys., 14, 9233–9247, doi:10.5194/acp-14-9233-2014, 2014.

Thornton, J. A. and Abbatt, J. P. D.: N_2O_5 reaction on submicron sea salt aerosol: Kinetics, products, and the effect of surface active organics, J. Phys. Chem. A, 109, 10004–10012, 2005.

Thornton, J. A., Braban, C. F., and Abbatt, J. P. D.: N_2O_5 hydrolysis on sub-micron organic aerosols: the effect of relative humidity, particle phase, and particle size, Phys. Chem. Chem. Phys., 5, 4593–4603, 2003.

Wachsmuth, M., Gäggeler, H. W., von Glasow, R., and Ammann, M.: Accommodation coefficient of HOBr on deliquescent sodium bromide aerosol particles, Atmos. Chem. Phys., 2, 121–131, doi:10.5194/acp-2-121-2002, 2002.

Wagner, C., Hanisch, F., Holmes, N., de Coninck, H., Schuster, G., and Crowley, J. N.: The interaction of N_2O_5 with mineral dust: aerosol flow tube and Knudsen reactor studies, Atmos. Chem. Phys., 8, 91–109, doi:10.5194/acp-8-91-2008, 2008.

Wahner, A., Mentel, T. F., Sohn, M., and Stier, J.: Heterogeneous reaction of N_2O_5 on sodium nitrate aerosol, J. Geophys. Res., 103, 31103–31112, 1998.